electronic reprint

Acta Crystallographica Section A
Foundations of Crystallography
ISSN 0108-7673
Editor: **D. Schwarzenbach**

The interplay between experiment and theory in charge-density analysis

Philip Coppens and Anatoliy Volkov

Acta Crystallographica Section A
Foundations of Crystallography
ISSN 0108-7673

Received 22 March 2004
Accepted 18 June 2004

The interplay between experiment and theory in charge-density analysis

Philip Coppens* and Anatoliy Volkov

Department of Chemistry, State University of New York at Buffalo, Buffalo, NY 14260-3000, USA. Correspondence e-mail: coppens@buffalo.edu

The comparison of theory and experiment remains a cornerstone of scientific inquiry. Various levels of such comparison applicable to charge-density analysis are discussed, including static and dynamic electron densities, topological properties, *d*-orbital occupancies and electrostatic moments. The advantages and drawbacks of the pseudoatom multipole are discussed, as are the experimentally constrained wavefunctions introduced by Jayatilaka and co-workers, which combine energy minimization with the requirement to provide a reasonable fit to the X-ray structure factors. The transferability of atomic densities can be exploited through construction of a pseudoatom databank, which may be based on analysis of *ab initio* molecular electron densities, and can be used to evaluate a host of physical properties. Partitioning of theoretical energies with the Morokuma–Ziegler energy decomposition scheme allows direct comparison with electrostatic interaction energies obtained from electron densities represented by the pseudoatom formalism. Compared with the Buckingham expression for the interaction between non-overlapping densities, the agreement with theory is much improved when a newly developed hybrid EP/MM (exact potential/multipole model) method is employed.

1. Introduction

The complementary nature of theory and experiment and the need to verify scientific hypotheses by experimental means has been a cornerstone of scientific inquiry since the end of the Middle Ages. According to popular lore, in 1612 Galilei dramatically refuted Aristotle's laws of motion, which stated that heavier objects fall faster in proportion to their weight than lighter objects, by dropping unequal weights from the Leaning Tower of Pisa (Fig. 1). However, in all his writings, Galileo never claimed to have conducted an experiment from that tower (Weiss, 1999). Apparently, the attribution to Galileo first appeared in the writings of his first biographer, Vincenzo Viviani, about a dozen years after Galileo's death. But such experiments were in fact conducted decades earlier, in 1586 by Stevin in The Netherlands and in 1597 by Mazzoni in Pisa. No matter to whom the experiments should be attributed (authorship was already an issue in those days!), the testing of theory by experiment introduced a new paradigm and remains a milestone in the history of science.

The charge or electron density is a fundamental observable, which (if known at infinite resolution) fully defines the ground-state properties of the system (Hohenberg & Kohn, 1964). Experimental charge-density studies, while off to a rocky start until experimental techniques and computational capabilities started to improve dramatically in the sixties, have advanced sufficiently to allow meaningful comparison with theoretical results. A schematic flow diagram of the experimental procedure, and comparison with theory at various levels, is shown in Fig. 2. Deformation density maps, obtained directly from experiment and/or after treatment of the data with an aspherical-atom scattering formalism that takes into account the bonding effects, are widely used. More sophisticated analysis may include (*a*) the topological local and integrated parameters of the electron density, (*b*) the electrostatic

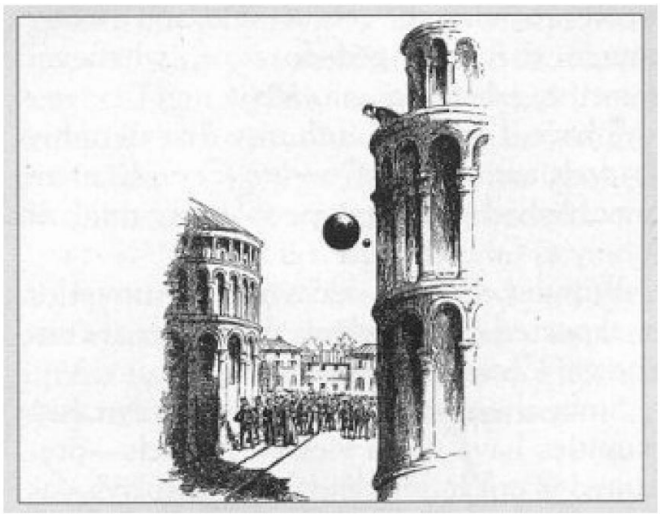

Figure 1
An early comparison of theory and experiment (from Weiss, 1999).

potential, electric field and its gradient calculated from the electron density, and (*c*) atomic and molecular electrostatic moments obtained with one of several well defined electron-density partitioning schemes. The latter can be used for calculation of intermolecular interactions and lattice energies, though these can also be obtained through direct integration of the electron density. How well are we doing at these various levels, what are the limitations and are there any areas where improvement is called for?

2. Direct comparison of experimental and theoretical electron densities

It is becoming increasingly recognized that the one-electron density is a central property that contains a wealth of information concerning the electronic structure of molecules and solids. One of the prime comparisons between theory and experiment is therefore at the electron-density level. The early work, almost exclusively based on the analysis of the *deformation density* in which a non-bonded reference state is subtracted to enhance the bonding features, demonstrated the feasibility and potential of the experimental approach. In more recent studies, the primary focus has shifted to the properties of the *total electron density*, as in the topological analysis within the concepts of Bader's atoms-in-molecules (AIM) theory (Bader, 1990).

However, the density as accessible experimentally is by definition time-averaged over both the internal and external vibrations. Thus, in the comparison of experimental and theoretical densities a choice must be made between either averaging the theoretical density or deconvoluting the thermal motion from the experimental results, each with its own drawbacks due to the need for a proper description of the vibrational modes of the system. The former approach was the first to be applied (Ruysink & Vos, 1974), as the deconvolution requires use of the aspherical-atom scattering model, which has only recently been fully developed. As the largest amplitudes of the thermal motion in molecular crystals are due to the low-frequency external modes, internal modes, which would require a series of calculations within the Born–Oppenheimer approximation, are typically neglected. The method requires thermal smearing to be applied to one- and two-center terms in the theoretical density expression, which can be done readily in the case of Gaussian basis functions (Stevens *et al.*, 1977). The deformation densities in the plane of the formamide molecule are shown in Fig. 3 (Stevens *et al.*,

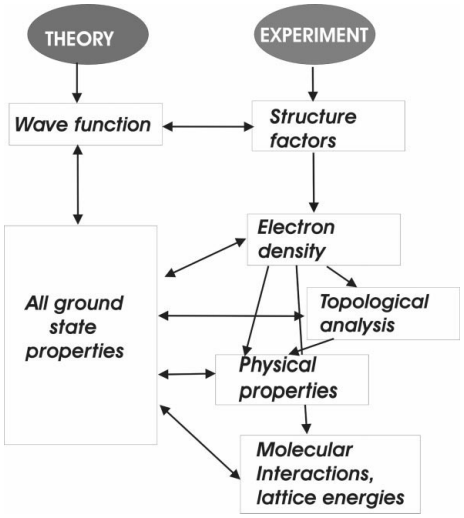

Figure 2
The interface between theory and experiment in charge-density studies.

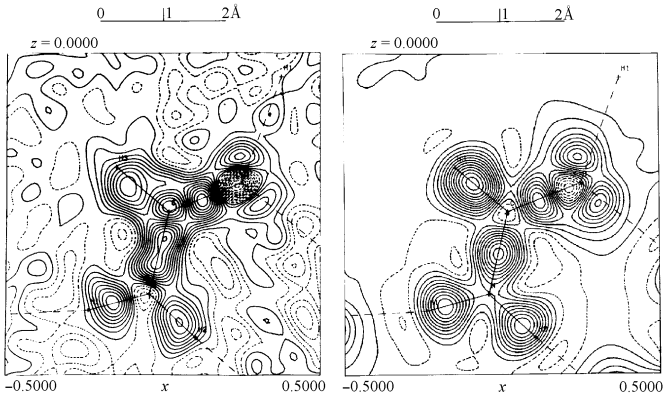

Figure 3
Experimental (left) and thermally smeared theoretical (right) deformation densities in the plane of the formamide molecule. Contours at 0.05 e Å^{-3}. Reprinted with permission from Stevens *et al.* (1978). Copyright (1978) American Chemical Society.

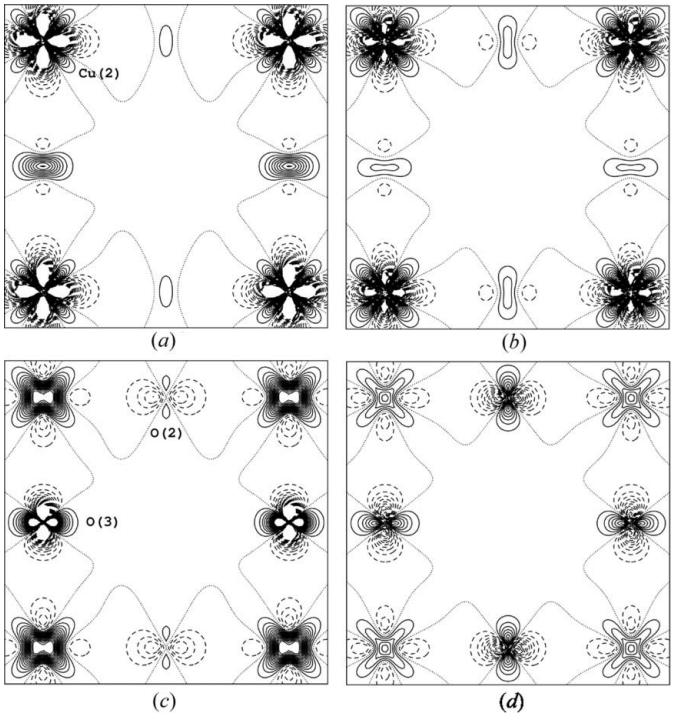

Figure 4
Deformation density for $YBa_2Cu_3O_{6.96}$ in planes parallel to (001). Positive contours solid, negative broken, zero contour dotted, contour interval 0.1 Å^{-3}, cut-off at 1.5 e Å^{-3}. (*a*, *b*: *z* = 0.355; *c*, *d*: *z* = 0.378); (*a*), (*c*) from multipole refinement of experimental structure factors; (*b*), (*d*) from multipole refinement of theoretical structure factors (from Lippmann *et al.*, 2003).

1978). While judged by today's standards the agreement would be considered rather poor, the comparison clearly shows that the main features are adequately reproduced.

In more recent studies, attention has shifted to the comparison of static densities, which involves deconvolution of the thermal-motion effect on the X-ray amplitudes. This procedure is being adopted even for extended solids in which thermal motion is generally much smaller than in molecular crystals. An example is a recent pioneering high-energy (99.49 keV, $\lambda = 0.124$ Å) synchrotron study on $YBa_2Cu_3O_{6.96}$ in which the experimental deformation density maps (Lippmann *et al.*, 2003) were compared with those calculated using the LAPW (linear augmented plane-wave) method implemented in the *WIEN2k* program (Blaha *et al.*, 2001). Two of the several sections calculated are reproduced in Fig. 4. The static maps, calculated from refinement of experimental and theoretical structure factors, respectively, show good agreement in the (001) plane reproduced in the figure, although some significant differences concerning the dipolar term on the O atoms and details of the distribution around the Cu atoms are found in other sections.

Fig. 5 gives a molecular crystal example. The experimental map in the plane of the *p*-nitroaniline molecule compares well with the theoretical PHF/6-31G** (PHF = periodic Hartree–Fock) deformation density, but even better with the same density obtained after projection of the PHF/6-31G** electron density onto the pseudoatom model through aspherical refinement of theoretical structure factors (Volkov *et al.*, 2000). Clearly, some of the differences between theory and experiment disappear by 'filtering' through the multipole formalism, especially close to the nuclei. As the experimental model- and multipole-refined theoretical maps are quite close, quantitative analysis of the corresponding physical properties is a logical next step.

In the comparison discussed above, differences between experimental and theoretical electron densities can also originate from the matrix effects if the crystal symmetry and periodicity are not included in the theoretical calculations (as, for example, in single-molecule calculations). These effects, while small, can in principle be detected by both experimental and theoretical methods (Spackman & Byrom, 1996). Fig. 6(*a*) shows the *interaction density* of the *p*-nitroaniline molecule in the neat crystal as calculated with the *CRYSTAL98* program (Dovesi *et al.*, 1998) with and without inclusion of intermolecular interactions. The interaction density is most pronounced in the substituent nitro and amine groups, which are involved in intermolecular (head-to-tail) hydrogen bonding; it reaches a level of 0.1 e Å^{-3}, which is well within the accuracy achievable with current experimental methods. Indeed, comparison of experimental electron densities of the *p*-nitroaniline molecule in the neat crystal and in the *p*-nitroaniline–18-crown-6 ether complex (Fig. 6*b*) shows the largest difference in the NO region of the molecule (Volkov, 2000), which is hydrogen bonded in the former but not in the latter crystal.

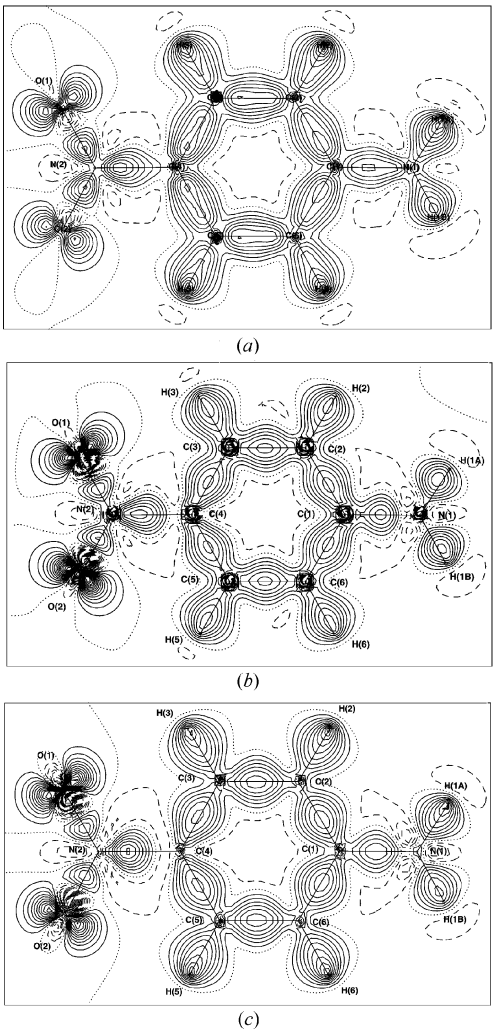

(*a*)

(*b*)

(*c*)

Figure 5
(*a*) Experimental map in the plane of the *p*-nitroaniline molecule. (*b*) The theoretical PHF/6-31G** (PHF = periodic Hartree–Fock) deformation density, and (*c*) PHF/6-31G** after refinement of theoretical structure factors $\sin\theta/\lambda \leq 1.05$ Å^{-1} (Volkov *et al.*, 2000).

3. Electrostatic moments in crystals

Since the comprehensive compilation of experimental electrostatic moments by Spackman (1992), much additional information has been extracted from experimental electron densities. The evidence points to an increase of the dipole moments through intermolecular polarization in the crystalline environment. Though the changes are sometimes too small to be detectable within experimental errors, many experimental and theoretical examples of dipole-moment enhancement have been reported [see for example 2-methyl-4-nitroaniline (Howard *et al.*, 1992), urea (Gatti *et al.*, 1994), ice VIII, formamide, urea (Spackman *et al.*, 1999), α-glycine (Destro *et al.*, 2000), phosphangulene (Madsen *et al.*, 2000) and references in these articles]. Interestingly, the effect can be pronounced even for weak C—H···O hydrogen bonds when a small amount of charge shifts across the hydrogen bond over a relatively large distance, as is the case in crystals of 3,4-bis(dimethylamino)-3-cyclobutene-1,2-dione (DMACB) (May *et al.*, 2001; Gatti *et al.*, 2002), which contain a very large

number of C—H···O contacts and no stronger competing interactions. Of a total of 23 C—H···O contacts in the crystal, 19 are classified as hydrogen-bonding interactions (Fig. 7) according to the criteria of Koch & Popelier (1995), as indicated by the presence or absence of a bond critical point. The collective effect of the weak interactions leads to an enhancement of the molecular dipole moment by about 70%, to more than 16 (1) D, compared with theoretical values of 7.30 D from isolated molecule calculations and ~12.7 D predicted by solid-state RHF/6-21-G theory. The dipole-moment increase is estimated to lead to a twofold increase of the molecular interaction energy in the crystal.

4. Transition-metal orbital occupancies

A useful interface between theory and experiment is the comparison of *d*-orbital occupancies of transition-metal complexes. In the case of transition metals, the overlap densities in the metal–ligand bonds are generally quite small so that the asphericity of the transition metal can be attributed to the preferential occupancy of the *d*-orbital levels. By equating the orbital description of the density with the density expressed in terms of the multipole algorithm, a set of equations is obtained from which the orbital occupancies can be derived (Holladay *et al.*, 1983). However, as orbitals are not uniquely defined, a choice of coordinate system is required, which is straightforward in highly symmetric coordination environments such as octahedral, tetrahedral, square-planar *etc*. In such cases, the agreement between theory and experiment is often quite satisfactory, as for example for the nickel squarate complex in the work by Wang and co-workers (Lee *et al.*, 1999). But in low-symmetry environments the choice of an appropriate coordinate system is not obvious. For Cu^{II}-alanylvaline, in which the d^9 Cu atom is in a distorted pentagonal site, for instance, the *d*-orbital cross terms vary dramatically with choice of the coordinate system (Sabino & Coppens, 2003). For symmetric complexes, orbital cross terms such as $d_{xy}d_{xz}$ in the density expression are small, or absent if dictated by crystallographic symmetry. Recognition of this feature provides a criterion that can be applied in the lower-symmetry cases. For Cu^{II}-alanylvaline, it is found that orienting the coordinate system such that the $d_{x^2-y^2}$ orbital population is minimized, which means that its *x* and *y* lobes

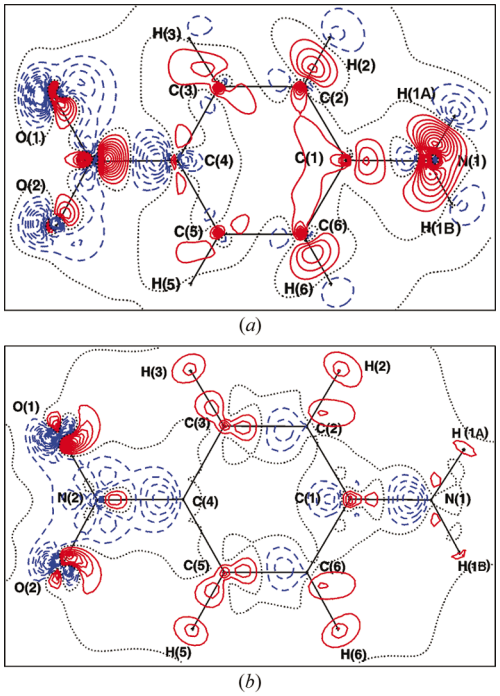

Figure 6
(*a*) Theoretical interaction density in the crystal of neat *p*-nitroaniline. Contours at 0.01 e Å^{-3} (Volkov, 2000). (*b*) Experimental difference density of *p*-nitroaniline molecule between the molecule in the neat crystal and its 18-crown-6 ether complex. Contours at 0.05 e Å^{-3} (Volkov, 2000).

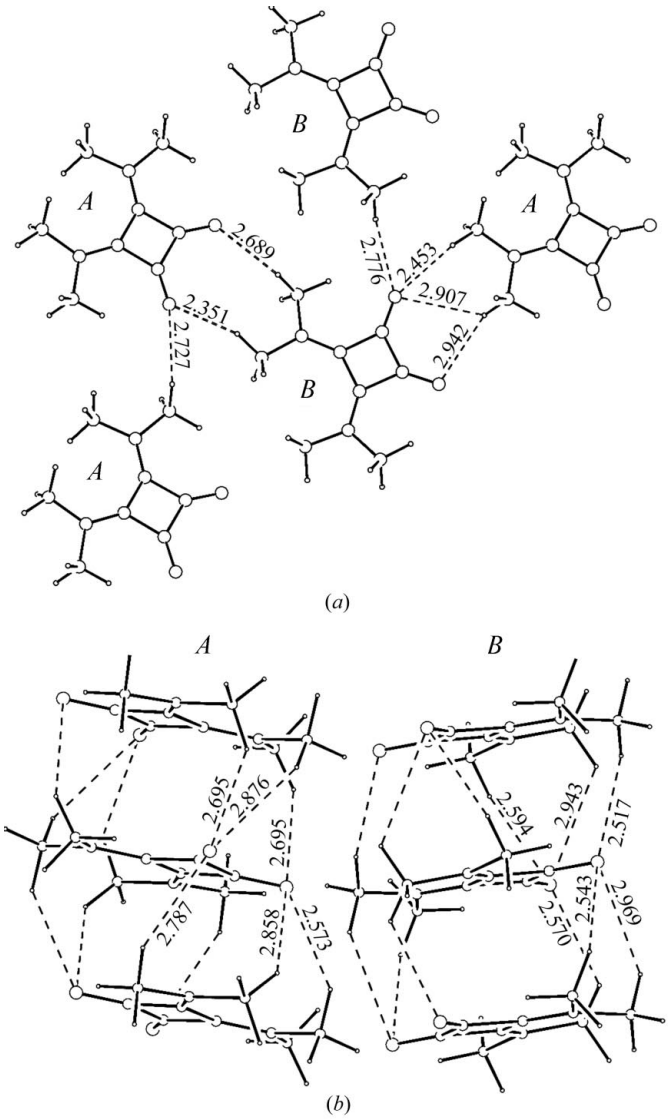

Figure 7
C—H···O intermolecular interactions (H···O < 3.0 Å) in DMACB crystals (*P* phase). Only the bonded interactions, as determined by the charge-density topology, are shown. (*a*) Intercolumn interactions. (*b*) Intracolumn interactions. Reprinted with permission from May *et al.* (2001). Copyright (2001) American Chemical Society.

optimally point to the ligand atoms, simultaneously minimizes the cross terms, and provides a well defined orientation, which can be used as a basis for comparison of theoretical and experimental results.

5. How good is the atom-centered multipole model?

It is appropriate to take a critical look at the aspherical-atom multipole (pseudoatom) model, as expressed in a number of algorithms (Hirshfeld, 1971, 1977*a*; Stewart, 1976), including the Hansen–Coppens model (Hansen & Coppens, 1978) employed in our own work. The pseudoatom model has significant advantages and its introduction has greatly contributed to the increasing application of experimental results in charge-density analysis:

(i) experimental noise is generally not fitted by the model functions and therefore effectively filtered out;

(ii) thermal motion is treated separately and deconvoluted from the final result;

(iii) the resulting static density provides an effective level of comparison with theoretical results, especially if the latter have been filtered through the model by refinement of theoretical structure factors;

(iv) notwithstanding the development of alternative formulations, including bond-charge models and orbital-based algorithms, no generally competitive alternative has been developed.

While the pseudoatom model is widely used in experimental density analysis, it is important not to lose sight of the implied assumptions.

(i) The results are dependent on the adequacy of the thermal motion formalism that is used (Mallinson *et al.*, 1988), which generally is limited to the harmonic approximation (but see Sørensen *et al.*, 2003). This is less of a drawback at the lowest achievable temperatures than at nitrogen or especially ambient temperature, at which anharmonic effects tend to be important and can correlate with the multipole description, especially when very high order data are not available. For the valence-only H atoms, correlation between the charge-density features and thermal motion is severe, unless reliable neutron data are available.[1]

(ii) The fine detail of the distribution is biased by the choice of the radial fit functions. This is especially true for the local properties of the electron density involving higher derivatives of the density, such as the Laplacian and its principal elements. Although differences between theory and experiment have occasionally been attributed to the effect of the crystal matrix, a more detailed analysis including solid-state and molecular calculations shows that a much more dominant contribution is due to the restricted functions into which the density is projected in the multipole model and in particular the limitation of the radial functions (Swaminathan *et al.*, 1984; Bianchi *et al.*, 1996; Volkov *et al.*, 2000). As noted, this is especially true for the bond-parallel (λ_3) curvatures along the bonds (Flaig *et al.*, 2002). A more flexible 'double-zeta' model is capable of reducing the discrepancy (Fig. 8) (Volkov & Coppens, 2001), but such models may contain too many correlated parameters to be useful with current quality X-ray data (Iversen *et al.*, 1997).

A note of caution concerning the above conclusions on the origin of the discrepancies is called for, as theoretical calculations are typically performed with Gaussian-type functions. Our recent studies of 'model' densities (Volkov, Li, Koritsanszky & Coppens, 2004; Volkov, unpublished results) show that the agreement between theory and experiment in the Laplacian, and especially the λ_3 curvature, can be much improved when the Slater-type functions are used in the wavefunction representation in theoretical calculations [as, for example, in the Amsterdam density functional program (te Velde *et al.*, 2001)].

The multipole model represents an extrapolation to infinite resolution from a finite set of experimental data. Sharp features, even those induced in the valence density by bonding effects, may not be represented in the multipole model maps as they will modify the X-ray scattering at higher Bragg angles only. The detailed structure near the atomic nuclei that is lacking in the multipole model deformation density maps (Fig. 5*c*) but present in the theoretical maps (Fig. 5*b*) is a result of this limitation.

Recent analysis of the radial behavior of the density functions based on the projection onto spherical harmonics (which are the angular functions in the multipole model) of either the total molecular densities directly calculated from high-quality

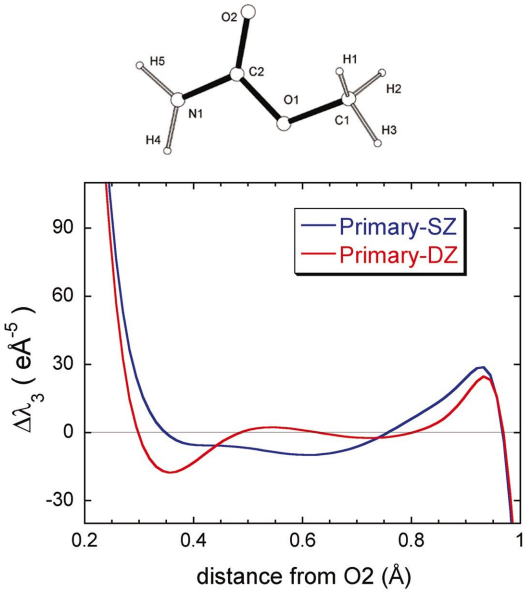

Figure 8
Difference in the l_3 profile along the O2—C2 bond in methyl carbamate for the SZ and DZ models relative to the values based on the original wavefunction (Volkov & Coppens, 2001).

[1] An attractive procedure aimed at circumventing this problem has been developed by Koritsanszky *et al.* (Flaig *et al.*, 1998). The mean-square displacements due to the internal modes are obtained from the frequencies of the energy-optimized isolated molecule as calculated with *ab initio* methods and transferred to the experimental molecular geometry. In the subsequent least-squares refinement, the shifts in the thermal parameters are restricted, *via* rigid-link-type constraints, to fulfill the rigid-body-motion requirement.

wavefunctions (Fernandez Rico *et al.*, 1999, 2002) or atomic fragments extracted from such densities (Koritsanszky & Volkov, 2004) provides a systematic way of improving the experimental multipole formalism. This is especially important for the weakly scattering H atom.

6. Experimentally restrained wavefunctions

According to the first Hohenberg–Kohn theorem, the ground-state properties of a many-electron system are uniquely defined by the electron density (Hohenberg & Kohn, 1964), though the functional relating the two is unknown. But the experimental density suffers from the limitations mentioned above, including that it (*a*) is only known at limited resolution, (*b*) is dependent on an inexact thermal motion model within the Born–Oppenheimer approximation, (*c*) is filtered through model functions and (*d*) is subject to experimental errors. Moreover, as pointed out by Jayatilaka & Grimwood (2001), the electron density is a continuous function and one would need an infinite number of measurements for its full determination. However, as shown by these authors, another approach may be followed, which consists of restraining the theoretical calculation to fit the experimental structure factors within reasonable bounds, keeping in mind the presence of experimental errors (Grimwood & Jayatilaka, 2001). Referred to by the authors as *experimental model wavefunctions*, or in brief *experimental wavefunctions*, these experimentally restrained wavefunctions offer an elegant use of the information available from experiment. Since the basis set in which the wavefunction is expressed can be very large, the model can be much more flexible than with experimental information alone. Furthermore, a successful treatment would give access to all available information, including the kinetic energy and properties depending on the two-electron density. Examples are the electron localization function (ELF) and the Fermi hole mobility function (FHMF) derived from experimentally restrained wavefunctions for ammonia, urea and alloxan (Jayatilaka & Grimwood, 2004). Although an estimate of the electron localization function (referred to as approximate ELF or AELF) has been obtained directly from the experimental density (Tsirelson & Stash, 2002) and is similar to the experimental-wavefunction-derived ELF with regard to the atomic shell structure, it contains artifacts resulting from the approximations made in its derivation (Tsirelson & Stash, 2002; Jayatilaka & Grimwood, 2004).

The need for a thermal motion formalism is not eliminated in the calculation of experimentally restrained wavefunctions, as a model must be used when applying the restraints. The method has also been applied to a HF calculation on a cluster of oxalic acid with four water molecules (Bytheway *et al.*, 2002), and seems equally applicable to crystal wavefunctions that are now theoretically accessible. The experimentally restrained wavefunction by necessity has a higher energy than achievable in the variational limit, the difference being dependent on the weights that are assigned to the experimental observations in the minimization procedure.

7. Electrostatic interaction energies

Given the electron density of each of two interacting bodies, the electrostatic interaction energy can be directly evaluated. One of the most convenient approaches is provided by the Buckingham algorithm (Buckingham, 1967), which is based on the approximation of non-overlapping densities. It expresses the interaction energy in terms of the electrostatic moments of each of the interacting molecules and has been generalized to be used with localized multipoles distributed over each of the bodies (Stone, 1981, 1997; Stone & Alderton, 1985). In the first evaluation of molecular interaction energies in crystals from experimental diffraction data, Spackman *et al.* combined the Buckingham method with the multipole expansion of the experimental densities of six different structures to obtain the electrostatic component of the interaction energy (Spackman *et al.*, 1988).

As the partitioning of a continuous electron distribution is not unique, the atomic moments can be defined in alternative ways: they can be (*a*) taken directly from the multipole model as in the work by Spackman *et al.* (1988), given the direct relation between the multipole populations and the atomic moments (Coppens, 1997), (*b*) derived from the Hirshfeld (stockholder) atoms (Hirshfeld, 1977*b*) calculated from the density, or (*c*) obtained from the atomic basins defined according to the concepts of the AIM theory (Bader, 1990). A recent study (Volkov & Coppens, 2004) examines in detail the accuracy of the intermolecular electrostatic interaction energies calculated with several types of atom-centered moments by comparing the resulting energies with those obtained from the Morokuma–Ziegler energy decomposition scheme (Morokuma, 1971; Kitaura & Morokuma, 1976; Ziegler & Rauk, 1977, 1979). The latter is available in the Amsterdam density functional (ADF) program (te Velde *et al.*, 2001) and has been extensively used for analysis of the nature of chemical bonds (Frenking *et al.*, 2003). To avoid the effect of experimental errors, theoretical molecular densities were used in the study by Volkov & Coppens (2004). While the stockholder and AIM moments were determined directly from the wavefunction-based electron density, the pseudoatom moments were obtained from the aspherical least-squares refinements of theoretical structure factors with $(\sin\theta/\lambda)_{\max} = 1.1$ Å^{-1}. The total intermolecular interaction energies were evaluated for 11 different types of dimers, as they occur in crystals of α-glycine, *N*-acetylglycine and (+)-L-lactic acid. It is found that the calculations with the Buckingham-type approximation in general underestimate the attractive electrostatic interactions. But the discrepancies are smaller for the AIM moments than for the other partitioning schemes, especially for dimers with short intermolecular contacts. This is understandable, as the non-overlap approximation is clearly valid for the discrete boundary AIM partitioning, but less appropriate for the 'fuzzy boundary' stockholder and pseudoatom treatments. Nevertheless, the relative strength of the electrostatic interactions is well reproduced by all partitioning methods. Representative results are given in Table 1. It is especially noticeable that Gavezzotti's energies for glycine

Table 1
Electrostatic interaction energies (kJ mol^{-1}) between monomers in the dimers occurring in crystals of α-glycine, *N*-acetylglycine and (+)-L-lactic acid (Volkov & Coppens, 2004; Volkov, Koritsanszky & Coppens, 2004) and results from double-zeta DFT calculations and the theoretical pseudoatom databank (Volkov, Li, Koritsanszky & Coppens, 2004).

G98 = *GAUSSIAN98* (Frisch *et al.*, 1998). For additional triple-zeta results, see the original literature.

	Morokuma–Ziegler	Stockholder moments		AIM moments		Pseudoatom moments only		EP/MM
Dimer	ADF	ADF	G98	ADF	G98	G98	Databank	Databank
Gly1	−108	−82	−92	−88	−94	−83	−84	−115
Gly2	−35	−15	−14	−15	−13	−10	−5	−27
Gly3	−102	−68	−82	−88	−96	−78	−81	−88
Gly4	−165	−130	−143	−138	−149	−134	−129	−162
Gly5	+35	+44	+52	+45	+52	+53	+52	+47
Gly6	−26	−20	−22	−23	−24	−20	−18	−23
AcG1	−47	−27	−27	−31	−29	−27	−29	−54
AcG2	−90	−63	−63	−88	−69	−30	−29	−93
Lac1	−63	−42	−45	−48	−46	−36	−26	−78
Lac2	−42	−26	−27	−24	−26	−21	−21	−41
Lac3	−14	−9	−9	−9	−9	−16	−15	−18

dimers using the 'pixel by pixel' SCDS (semiclassical density sum) method (Gavezzotti, 2002, 2003*a*,*b*,*c*) agree very well with the Morokuma–Ziegler energy decomposition results listed in the first column of Table 1.

To eliminate the shortcomings of the Buckingham approximation, which is not valid for overlapping densities as occur at short interatomic distances, a new method was developed. In the EP/MM (exact potential/multipole model) method, the electrostatic interactions between pairs of atoms within a certain critical distance (typically 4 Å) are treated exactly, while the rapid Buckingham calculation is performed for larger internuclear separations (Volkov, Li, Koritsanszky & Coppens, 2004). Dramatic improvements of up to 60 kJ mol^{-1} in the electrostatic interaction energies are obtained for the pseudoatom model, the improvements being especially pronounced for dimers with short intermolecular contacts. As illustrated by comparison of the first and the last columns of Table 1, with the EP/MM method the pseudoatom results give a very good agreement with Morokuma–Ziegler electrostatic energies that is comparable or better than the agreement obtained with the AIM moments.

8. The use of a databank of transferable atoms

To obtain the interaction energies for macromolecules, for which adequate crystals are generally not available and theoretical methods become necessarily approximate, the transferability of the pseudoatoms can be exploited to great advantage. A databank of experimental pseudoatoms based on charge-density studies on a series of oligopeptides has been pioneered by Pichon-Pesme and Lecomte and co-workers (Wiest *et al.*, 1994; Pichon-Pesme *et al.*, 1995; Jelsch *et al.*, 1998). While such a databank incorporates the effects of intermolecular interactions, they must by necessity be averaged over the differing environments of the structures on which the databank is based. An alternative approach, which eliminates the effect of experimental errors but may be subject to theoretical approximations, is to base the databank of transferable pseudoatoms on theoretical densities (Koritsanszky *et al.*, 2002). A theoretical databank can be fairly rapidly constructed and allows incorporation of diverse atom types. Such a databank based on DFT densities has been constructed, and the first results are now available (Volkov & Coppens, 2004; Volkov, Li, Koritsanszky & Coppens, 2004; Volkov, Koritsanszky & Coppens, 2004). As shown in Table 1, the databank gives very consistent results for the electrostatic interaction energies, of a quality comparable to those obtained with the primary densities. Similar results are obtained for dimers of glutamine, serine and leucine (Volkov, Li, Koritsanszky & Coppens, 2004). The excellent transferability of the theoretical pseudoatoms is further demonstrated by the agreement between primary and databank densities for integrated and local electron-density properties, including the electrostatic potential, net atomic charges and higher atomic moments, curvatures along the bond path (λ_3) and in the perpendicular plane (λ_1 and λ_2), the Laplacian and the displacement of the bond critical points from the bond midpoints.

The good-quality densities that can be readily constructed from a databank of aspherical pseudoatoms sets new standards for future charge-density studies, which even more than before should concentrate on unusual bonding situations, the effects of interactions between molecules, on metastable states and, in the more distant future, on short-lived transient species.

9. Concluding remarks

We have discussed the comparison of experimental and theoretical electron densities at different levels, including *d*-orbital occupancies, molecular moments, topological properties and electrostatic interaction energies as well as the comprehensive theoretical–experimental treatment pioneered by Jayatilaka and co-workers. The interaction between theory and experiment in charge-density research continues to be a crucial component of the field.

Finally, we would like to note that many other high-quality studies have been reported that could not be included in this brief essay.

Support by the National Institutes of Health (GM56829) and the National Science Foundation (CHE0236317) is gratefully acknowledged.

References

Bader, R. F. W. (1990). *Atoms in Molecules. A Quantum Theory*. New York: Oxford University Press.

Bianchi, R., Gatti, C., Adovasio, V. & Nardelli, M. (1996). *Acta Cryst.* B**52**, 471–478.

Blaha, P., Schwarz, K., Madsen, G., Kvasnicka, D. & Luitz, J. (2001). *WIEN2k, an Augmented Plane Wave + Local Orbitals Program for Calculating Crystal Properties*. K. Schwarz, TU Wien, Austria. ISBN 3-9501031-1-2.

Buckingham, A. D. (1967). *Adv. Chem. Phys.* **12**, 107.

Bytheway, I., Grimwood, D. J. & Jayatilaka, D. (2002). *Acta Cryst.* A**58**, 232–243.

Coppens, P. (1997). *X-ray Charge Densities and Chemical Bonding*, pp. 147–149. New York: Oxford University Press.

Destro, R., Roversi, P., Barzaghi, M. & Marsh, R. E. (2000) *J. Phys. Chem. A*, **104**, 1047–1054.

Dovesi, R., Saunders, V. R., Roetti, C., Causà, M., Harrison, N. M., Orlando, R. &. Zicovich-Wilson, C. M. (1998). *CRYSTAL98 User's Manual*. University of Torino, Italy.

Fernandez Rico, J., Lopez, R., Ema, I. & Ramyrez, G. (2002). *J. Chem. Phys.* **117**, 533–540.

Fernandez Rico, J., Lopez, R. & Ramyrez, G. (1999). *J. Chem. Phys.* **110**, 4213–4220.

Flaig, R., Koritsanszky, T., Dittrich, B., Wagner, A. & Luger, P. (2002). *J. Am. Chem. Soc.* **124**, 3407–3417.

Flaig, R., Koritsanszky, T., Zobel, D. & Luger, P. (1998) *J. Am. Chem. Soc.* **120**, 2227–2238.

Frenking, G., Wichmann, K., Fröhlich, N., Loschen, C., Lein, M., Frunzke, J. & Rayón, V. M. (2003). *Coord. Chem. Rev.* **238–239**, 55–82.

Frisch, M. J., Trucks, G. W., Schlegel, H. B., Gill, P. M., Johnson, B. G., Robb, M. A., Cheeseman, J. R., Keith, T., Petersson, G. A., Montgomery, J. A., Raghavachari, K., Al-Laham, M. A., Zakrzewski, V. G., Ortiz, J. V., Foresman, J. B., Cioslowski, J., Stefanov, B. B., Nanayakkara, A., Challacombe, M., Peng, C. Y., Ayala, P. Y., Chen, W., Wong, M. W., Andres, J. L., Replogle, E. S., Gomperts, R., Martin, R. L., Fox, D. J., Binkley, J. S., Defrees, D. J., Baker, J., Stewart, J. P., Head-Gordon, M., Gonzalez, C., Pople, J. A. (1998). *GAUSSIAN98*, Revision A.8. Gaussian Inc., Pittsburgh, PA, USA.

Gatti, C., May, E., Destro, R. & Cargnoni, F. (2002). *J. Phys. Chem.* A**106**, 2707–2720.

Gatti, C., Saunders, V. R. & Roetti, C. (1994). *J. Chem. Phys.* **101**, 10686–10696.

Gavezzotti, A. (2002). *J. Phys. Chem.* **106**, 4145–4154.

Gavezzotti, A. (2003*a*). *J. Phys. Chem.* **107**, 2344–2353.

Gavezzotti, A. (2003*b*). *Cryst. Eng. Commun.* **5**, 429–438.

Gavezzotti, A. (2003*c*). *Cryst. Eng. Commun.* **5**, 439–446.

Grimwood, D. J. & Jayatilaka, D. (2001). *Acta Cryst.* A**57**, 87–100.

Hansen, N. K. & Coppens, P. (1978). *Acta Cryst.* A**34**, 909–921.

Hirshfeld, F. L. (1971). *Acta Cryst.* B**27**, 769–781.

Hirshfeld, F. L. (1977*a*). *Isr. J. Chem.* **16**, 226–229.

Hirshfeld, F. L. (1977*b*). *Theor. Chim. Acta*, **44**, 129–138.

Hohenberg, P. & Kohn, W. (1964). *Phys. Rev. B*, **136**, 864–871.

Holladay, A., Leung, P. C. & Coppens, P. (1983). *Acta Cryst.* A**39**, 377–387.

Howard, S. T., Hursthouse, M. B., Lehmann, C. W., Mallinson, P. R. & Frampton, C. S. (1992). *J. Chem. Phys.* **97**, 5616–5630.

Iversen, B. B., Larsen, F. K., Figgis, B. N. & Reynolds, P. A. (1997). *J. Chem. Soc. Dalton Trans.* pp. 2227–2240.

Jayatilaka, D. & Grimwood, D. J. (2001). *Acta Cryst.* A**57**, 76–86.

Jayatilaka, D. & Grimwood, D. J. (2004). *Acta Cryst.* A**60**, 111–119.

Jelsch, C., Pichon-Pesme, V., Lecomte, C. & Aubry, A. (1998). *Acta Cryst.* D**54**, 1306–1318.

Kitaura, K. & Morokuma, K. (1976). *Int. J. Quantum Chem.* **10**, 325–340.

Koch, U. & Popelier, P. L. A. (1995). *J. Phys. Chem.* **99**, 9747–9754.

Koritsanszky, T. & Volkov, A. (2004). *Chem. Phys. Lett.* **385**, 431–434.

Koritsanszky, T., Volkov, A. & Coppens P. (2002). *Acta Cryst.* A**58**, 464–472.

Lee, C.-H., Wang, C.-C., Chen, K.-C., Lee, G.-H. & Wang, Y. (1999). *J. Phys. Chem. A*, **103**, 156–165.

Lippmann, T., Blaha, P., Andersen N. H., Poulsen, H. F., Wolf, T., Schneider, J. R. & Schwarz, K.-H. (2003). *Acta Cryst.* A**59**, 437–451.

Madsen, G. K. H., Krebs, F. C., Lebech, B. & Larsen, F. K. (2000). *Chem. Eur. J.* **6**, 1797–1804.

Mallinson, P. R., Koritsanszky, T., Elkaim, E., Li, N. & Coppens, P. (1988). *Acta Cryst.* A**44**, 336–342.

May, E., Destro, R. & Gatti, C. (2001). *J. Am. Chem. Soc.* **123**, 12248–12252.

Morokuma, K. (1971). *J. Chem. Phys.* **55**, 1236–1244.

Pichon-Pesme, V., Lecomte, C. & Lachekar, H. (1995). *J. Phys. Chem.* **99**, 6242–6250.

Ruysink, A. F. J. & Vos, A. (1974). *Acta Cryst.* A**30**, 497–502.

Sabino, J. R. & Coppens, P. (2003). *Acta Cryst.* A**59**, 127–131.

Sørensen, H. O., Stewart, R. F., McIntyre, G. J. & Larsen, S. (2003). *Acta Cryst.* A**59**, 540–550.

Spackman, M. A. (1992). *Chem. Rev.* **92**, 1769–1797.

Spackman, M. A. & Byrom, P. G. (1996). *Acta Cryst.* B**52**, 1023–1035.

Spackman, M. A., Byrom, P. G., Alfredsson, M. & Hermansson, K. (1999). *Acta Cryst.* A**55**, 30–47.

Spackman, M. A., Weber, H. P. & Craven, B. M. (1988). *J. Am. Chem. Soc.* **110**, 775–782.

Stevens, E. D., Rys, J. & Coppens, P. (1977). *Acta Cryst.* A**33**, 333–338.

Stevens, E. D., Rys, J. & Coppens, P. (1978). *J. Am. Chem. Soc.* **100**, 2324–2328.

Stewart, R. F. (1976). *Acta Cryst.* A**32**, 565–574.

Stone, A. J. (1981). *Chem. Phys. Lett.* **83**, 233–239.

Stone, A. J. (1997). *The Theory of Intermolecular Forces*. New York: Oxford University Press.

Stone, A. J. & Alderton, M. (1985). *Mol. Phys.* **56**, 1047–1064.

Swaminathan, S., Craven, B. M., Spackman, M. A. & Stewart, R. F. (1984). *Acta Cryst.* B**40**, 398–404.

Tsirelson, V. & Stash, A. (2002). *Chem. Phys. Lett.* **351**, 142–148.

Velde, G. te, Bickelhaupt, F. M., van Gisbergen, S. J. A., Fonseca Guerra, C., Baerends, E. J., Snijders, J. G. & Ziegler, T. J. (2001). *J. Comput. Chem.* **22**, 931–967.

Volkov, A. V. (2000). PhD thesis, State University of New York at Buffalo, New York, USA.

Volkov, A., Abramov, Y., Coppens, P. & Gatti, C. (2000). *Acta Cryst.* A**56**, 332–339.

Volkov, A. & Coppens, P. (2001). *Acta Cryst.* A**57**, 395–405.

Volkov, A. & Coppens, P. (2004). *J. Comput. Chem.* **25**, 921–934.

Volkov, A., Koritsanszky, T. S. & Coppens, P. (2004) *Chem. Phys. Lett.* **391**, 170–175.

Volkov, A., Li, X., Koritsanszky, T. & Coppens, P. (2004). *J. Phys. Chem. A*, **108**, 4238–4300.

Weiss, P. (1999). http://www.endex.com/gf/buildings/ltpisa/ltpnews/1999/ltpsn121899.htm.

Wiest, R., Pichon-Pesme, V., Benard, M. & Lecomte, C. (1994). *J. Phys. Chem.* **98**, 1351–1362.

Ziegler, T. & Rauk, A. (1977). *Theor. Chim. Acta*, **46**, 1–10.

Ziegler, T. & Rauk, A. (1979). *Inorg. Chem.* **18**, 1755–1759.